AIM AND APPROACH

Here, we propose a double-sided passivation strategy by introducing phenylethyl ammonium iodide (PEAI) at the top and bottom wide bandgap perovskite interfaces. We elucidated the subtle chemical interaction between PEAI, perovskite and NiO_x through theory and experiment. The result proves that this chemical interaction can further improve the quality of the perovskite film, thereby reducing the bulk nonradiative recombination of the device and strengthening interface connections. In addition, the reduced interface defects also lead to reduced non-radiative recombination at the interface. Ultimately, single-junction wide bandgap PSCs achieved a high PCE of 16.5%, while device stability improved. The PEAI-based all-perovskite tandem solar cell also got a champion PCE of 26.81%.

EXPERIMENTS AND METHODS

ITO glasses were ultrasonically cleaned for 20 minutes in sequence with detergent water and isopropyl alcohol. Then the ITO was treated for 5 minutes with plasma. Then the glasses were transformed into the glove box. 20 mg NiOx was dissolved in 1 ml water and stirring 10 min at room temperature. Then the NiOx was spin-coated on the ITO with the speed of 4000 rpm for the 30 s, followed by annealing at 100 °C for 10 minutes. For bottom PEAI modification: 1 mg of PEAI were dissolved in 1 ml IPA and this solution was spin-coated on the NiOx at a speed of 5000 rpm for the 30 s. Then the substrate was put on the hot stage at a temperature of 100 °C for 10 minutes. The perovskite precursor solution was prepared by dissolving FAI (99.05 mg), CsI (37.41 mg), FABr (47.98 mg), PbI_2 (331.93 mg), $PbBr_2$ (176.16 mg), and CsBr (20.43 mg) in 1 mL of DMSO / DMF (1/4, v/v) mixture. The perovskite film was deposited using the two-step spin-coating method at 2000 rpm for 10 seconds and 6000 rpm for the 40s, with 150 μL of CB anti-solvent dripped over perovskite films for 30 seconds before the program was terminated, and the film was subsequently annealed at 100 °C for 10 minutes. For top PEAI modification: 1mg / mL PEAI was dissolved in IPA, and then was spin-coated on the perovskite film at a speed of 5000 rpm for the 30 s. Then the substrate was put on the hot stage at a temperature of 100 °C for 10 minutes. After cooling to room temperature, the substrates were transferred to the evaporation system. Finally, C_{60} (20 nm), BCP (7 nm), and Ag (100 nm) were sequentially deposited on top of the perovskite by thermal evaporation under a vacuum of 5×10^{-5} Pa through using a shadow mask.

RESULTS AND DISCUSSION

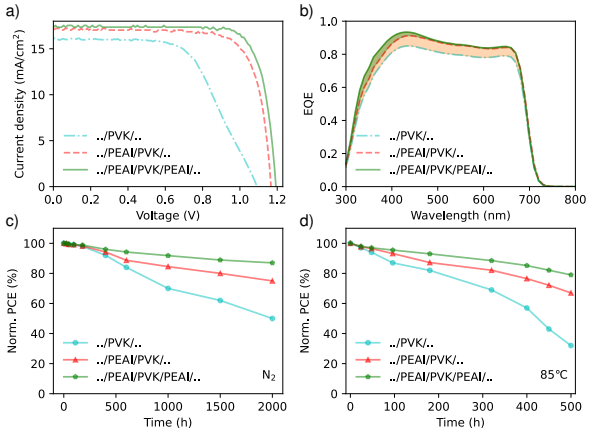

FIGURE 1. (a) *J-V* curves and (b) EQE spectra of the device with or without PEAI modification. (c) N_2 and (d) thermal stability of unpackaged devices which stored in N_2-filled glove box.

Figure 1a shows the typical *J-V* curves of the device with or without PEAI modification. The corresponding photovoltaic parameters are listed in Table 1. The champion control device has a PCE of 10.72%, the bottom-modification

TABLE 1. Photovoltaic parameters of the champion control, bottom and both-modification devices measured under simulated AM 1.5G one sun illumination of 100 mW cm^{-2}.

Device	J_{SC} [mA cm^{-2}]	V_{OC} [V]	FF [%]	PCE [%]
Control[a]	16.12	1.085	61.3	10.72
Bottom[b]	17.22	1.165	77.1	15.46
Both[c]	17.35	1.192	79.2	16.37

[a] ITO/NiO_x/PVK/C_{60}/BCP/Ag. [b] ITO/NiO_x/PEAI/PVK/C_{60}/BCP/Ag. [c] ITO/NiO_x/PEAI/PVK/PEAI/C_{60}/BCP/Ag.

device shows a PCE of 15.46%, and both-modification devices have a PCE of 16.37%. The external quantum efficiency (EQE) result shows the three typical devices' integrated current density, which was in good agreement with those obtained from *J-V* curves (Figure 1b). The stability of the device with or without PEAI modification was further tested and shown in Figure 1c-d. Figure 1c shows the long-term stability of the unencapsulated control and target devices aged under the N_2 glovebox. After ageing for 2000 h, the control device maintained 50% of its initial PCE, the PEAI/PVK device retained 75% of its original PCE, while the both-modification device retained 87% of its original PCE. The thermal stability of the unsealed control and target devices aged at 85 °C in the dark and the N_2-filled glovebox is exhibited in Figure 1d. At least 79% of its initial PCE was maintained for the target device after ageing for 500 h, whereas only 32% was maintained for the control device.

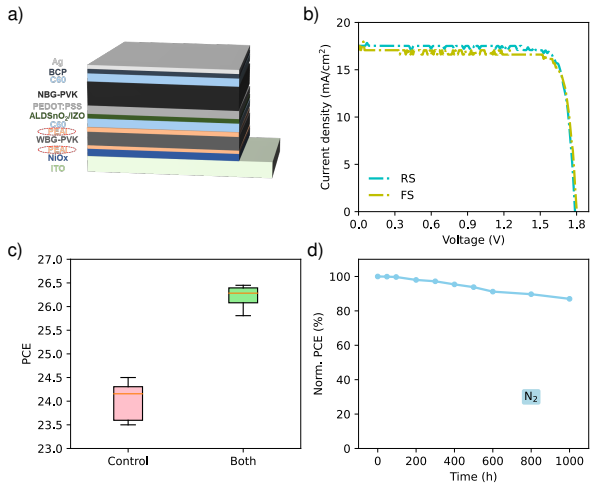

FIGURE 2. (a) Schematic illustration of the tandem solar cell structure in this work. (b) *J-V* curves of the device with PEAI co-modification. (c) PCE statistics of the tandem PSCs with or without PEAI co-modification. (d) long-term stability of unpackaged tandem solar cells.

Then, we fabricated the perovskite/perovskite tandem solar cell to prove the potential of the PEAI on tandem solar cells further. As shown in Figure 2a, the structure of ITO/NiO_x/(PEAI)/WBG perovskite/(PEAI)/C_{60}/ALD SnO_2/IZO/PEDOT:PSS/NBG perovskite/C_{60}/BCP/Ag was designed in this work. The typical *J-V* curves of the best-performing tandem solar cells with PEAI modification are shown in Figure 2b. After using PEAI, we can get a high PCE of 26.81% with a J_{SC} of 17.98 mA cm^{-2}, a V_{OC} of 1.79 V, and an FF of 0.833. Figure 2c presents the statistical results of the tandem solar cells with or without PEAI modification. As we can see that the both-PEAI modified devices show a high average PCE compared with the control devices. Finally, the stability of the tandem solar cells was tested in a glovebox filled with N_2. As shown in Figure 2d, the PEAI-based device maintained 87% of its initial PCE after ageing for 1000 h.

CONCLUSION

In summary, we propose a universal passivation strategy: co-interface collaborative passivation. By introducing PEAI, the quality of the perovskite film was improved, and the bulk nonradiative recombination of the film was reduced. At the same time, the interface connection of the film was strengthened through strong chemical interaction, and the surface defects of the film were passivated, thereby further reducing the interface nonradiative recombination of the device. The DFT results further prove the experimental conclusions. In the end, the efficiency of single-junction PSCs based on the co-modification strategy reached 16.5%, while the efficiency of all-perovskite tandem solar cells reached 26.81%. This work provides guidance for developing co-modifications strategies while supporting further commercialization of perovskite solar cells.

REFERENCES

1. H. Bi, Y. Guo, M. Guo, C. Ding, S. Hayase, H. Zou, Q. Shen, G. Han, W. Hou, *J. Power Sources* **2023**, *563*, 232825.
2. H. Bi, G. Han, M. Guo, C. Ding, S. Hayase, H. Zou, Q. Shen, Y. Guo, W. Hou, *Sol. RRL* **2022**, *6*, 2200352.
3. H. Bi, J. Liu, Z. Zhang, L. Wang, R. Beresneviciute, D. Tavgeniene, G. Kapil, C. Ding, A. K. Baranwal, S. R. Sahamir, Y. Sanehira, H. Segawa, S. Grigalevicius, Q. Shen, S. Hayase, *ACS Energy Lett.* **2023**, *8*, 3852.
4. J.-F. Guillemoles, T. Kirchartz, D. Cahen, U. Rau, *Nat. Photonics* **2019**, *13*, 501.
5. Q. Han, Y. Wei, R. Lin, Z. Fang, K. Xiao, X. Luo, S. Gu, J. Zhu, L. Ding, H. Tan, *Sci. Bull.* **2019**, *64*, 1399.
6. R. He, S. Ren, C. Chen, Z. Yi, Y. Luo, H. Lai, W. Wang, G. Zeng, X. Hao, Y. Wang, J. Zhang, C. Wang, L. Wu, F. Fu, D. Zhao, *Energy Environ. Sci.* **2021**, *14*, 5723.
7. S. Hu, K. Otsuka, R. Murdey, T. Nakamura, M. A. Truong, T. Yamada, T. Handa, K. Matsuda, K. Nakano, A. Sato, K. Marumoto, K. Tajima, Y. Kanemitsu, A. Wakamiya, *Energy Environ. Sci.* **2022**, *15*, 2096.
8. L. Krückemeier, U. Rau, M. Stolterfoht, T. Kirchartz, *Adv. Energy Mater.* **2019**, *10*, 1902573.
9. C. Li, Y. Zhang, X. Zhang, P. Zhang, X. Yang, H. Chen, *Adv. Funct. Mater.* **2023**, *33*, 2214774.
10. NREL, Best Research-Cell Efficiency Chart **2023-09-30**.
11. J. Tian, K. Zhang, Z. Xie, Z. Peng, J. Zhang, A. Osvet, L. Lüer, T. Kirchartz, U. Rau, N. Li, C. J. Brabec, *ACS Energy Lett.* **2022**, *7*, 4071.
12. S. P. Dunfield, L. Bliss, F. Zhang, J. M. Luther, K. Zhu, M. F. A. M. van Hest, M. O. Reese, J. J. Berry, *Adv. Energy Mater.* **2020**, *10*, 1904054.